Heliyon 10 (2024) e33726

Contents lists available at ScienceDirect

Heliyon

journal homepage: www.cell.com/heliyon

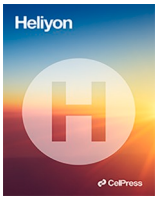

Research article

Sustainability assessment of machining Al 6061-T6 using Taguchi-grey relation integrated approach

Sajid Raza Zaidi [a], Shahid Ikramullah Butt [a], Muhammad Ali Khan [a,b,*], Muhammad Iftikhar Faraz [c], Syed Husain Imran Jaffery [a], Jana Petru [d]

[a] School of Mechanical and Manufacturing Engineering (SMME), National University of Sciences and Technology (NUST), Islamabad 44000, Pakistan
[b] Department of Mechanical Engineering, College of Electrical and Mechanical Engineering (CEME), National University of Sciences and Technology (NUST), Islamabad 44000, Pakistan
[c] Department of Mechanical Engineering, College of Engineering, King Faisal University, Al-Ahsa 31982, Saudi Arabia
[d] Department of Machining, Assembly and Engineering Metrology, Mechanical Engineering Faculty, VŠB-Technical University of Ostrava, 17, Listopadu 2172/15, Ostrava 708 00, Czech Republic

ARTICLE INFO

Keywords:
Al 6061-T6
Specific cutting energy
Process optimisation
Grey relational analysis
Sustainable manufacturing
Clean materials
Betterment of society

ABSTRACT

Modern machining requires reduction in energy usage, surface roughness, and burr width to produce finished or near-finished parts. To ensure high surface quality in machining processes, it is crucial to minimize surface finish and minimize burr width, which are considered as significant parameters as specific cutting energy. The objective of this study was to identify the optimal machining parameters for milling in order to minimize surface roughness, burr width, and specific cutting energy. To achieve this, the research investigated the impact of feed per tooth, cutting speed, depth of cut, and number of inserts on the responses across three intervals using Taguchi L9 array. Observing the responses by varying these parameters, underlined the need for multi objective optimisation. Machining conditions of 0.14 mm/tooth f_z, 350 m/min V_c and 2 mm *ap* using 1 cutting insert (exp no 9) was identified as the best machining run using grey relational analysis owing to its highest grey relational grade of 0.936. ANOVA examination identified cutting speed as the leading factor impacting the grey relational grade with 31.07 % contribution ratio, with the number of inserts, depth of cut, and feed per tooth also making notable contributions. Conclusively, machining parameters identified through response surface optimisation resulted in 21.69 % improvement in surface finish, 11.39 % reduction in specific energy consumption, and 6.2 % decrease in burr width on the down milling side albeit with an increase of 9 % in burr width on the up-milling side.

1. Introduction

Milling is a widely and frequently used machining process which can produce a variety of shapes, reducing costs and increasing production rates. Factors affecting cost and production rate include tool wear, management cost, and the production of finished or close to finished parts [1–3] Variable machining parameters such as cutting width, depth and speed, tool material, number of cutting

* Corresponding author. Department of Mechanical Engineering, College of Electrical and Mechanical Engineering (CEME), National University of Sciences and Technology (NUST), Islamabad 44000, Pakistan
E-mail address: mak.ceme@ceme.nust.edu.pk (M.A. Khan).

https://doi.org/10.1016/j.heliyon.2024.e33726
Received 23 June 2024; Accepted 26 June 2024
Available online 29 June 2024

teeth (inserts), type of lubricant [4,5], inserts geometry, feed rate, cutting tool path, and tool diameter [6,7] impact energy consumption [8], surface roughness [9,10], tool wear [11], and burr formation [12].

Minimum cost and maximum production rate have been a goal since 1950 [13], and machining systems in terms of energy are usually less efficient [14–17], with reported inefficiency levels of as low as 30 % [18,19]. Currently, only 14 % of the energy consumed during milling is used for material removal [20]. The total energy consumption, efficiency, and specific energy consumption of a machining operation depend upon the cutting parameters [21]. Optimisation of the cutting tool, tool path, and machining parameters can improve sustainability by up to 40 % [22]. During a milling operation, the key factors affecting specific cutting energy and power consumption are tool diameter, number of cutting inserts, and material removal rate (*MRR)* [4,23]. *MOO* (*MRR*) in milling operations can be achieved with multiple cutting tools and parameters, but the prediction of specific energy consumption (*SCE*) relies on feed rate, depth (*ap*), width and speed of cut (V_c) [24]. Reports in the literature show that impact on energy consumption during a milling operation is mainly dependant on depth, width and V_c [25–31]. Energy expenditure can be reduced by selecting appropriate machining parameters, leading to lower manufacturing costs and a competitive advantage [32–35].

Surface finish is one of the key parameters of dimensional accuracy [36], and surface roughness (R_a) has a large impact on the mechanical properties such as tensile strength [37], fatigue life, and surface topography [38]. Geometric factors, workpiece material, and machine tool vibrations are the three primary influences on the surface finish of machined parts [39]. To attain the desired surface finish, it is crucial to use appropriate machining parameters, including the type of operation, feed rate, and cutting tool geometry. However, achieving the desired surface finish is subject to the machinability of the workpiece and the work material factor, which also need to be taken into account [40–43]. Decreasing feed per tooth (f_z) and *ap* and increasing spindle speed and tool tip radius during the milling of SKD61 steel will result in improved surface finish [44]. Additionally, when dry milling aluminium alloy Al2041-T6, relief angles, concavity, V_c and feed rate were found to be significant factors affecting R_a [45]. Also, a considerable difference between surface quality of aluminium 6061-T6 under flood cooling and *MQL* conditions has been noticed [46]. It can thus be concluded that the selection of geometric factors such as feed rate, *ap*, width of cut, V_c and type of cutting operation can be used to optimize [10], improve [47–49] and predict [50,51] the surface finish of any machined part.

Burr formation and its underlying mechanisms has been widely researched in relation to milling [47,52,53], drilling [14,54–56], and other machining operations on various materials [57,58]. Milling operations tend to produce burrs at the points of contact between the workpiece and cutters [59,60] with smaller burrs typically existing on the up-milling side [61,62]. This is due to the cutting velocity being higher on the up-milling side than on the down-milling side [63]. The lower intensity of burrs on the up-milling side is attributed to the frictional forces of the tool sliding alongside the burr and getting stuck on the mill's flutes [64]. In a study of micro-milling titanium, it was found that f_z was the most influential machining parameter when it came to affecting burr width while *ap* had a negligible contribution. Additionally, lower spindle speeds led to a decrease in burr width [52]. A study on Niomic 75 revealed that using an uncoated tool result in larger burrs than a coated tool [65]. An experimental study on milling aluminium Al 2124 demonstrated that an increase in *ap* leads to larger burrs [66]. Kumar et al. [67] reported that burr formation is a complex process and depends on tool geometry, coatings, workpiece material properties, and cutting conditions.

Recent advances in technique have enabled more energy-efficient production of near-finished parts, with optimised machining responses achievable through optimised machining parameters. Studies suggest that width of cut and *ap* have the greatest effect on *SCE*, while spindle speed has the most significant impact on production rate [68]. Optimisation of machining parameters and cutting tools has been demonstrated to reduce carbon footprints, while simultaneously minimising production time [69]. Utilizing Grey relational analysis (*GRA*), a study had successfully attained up to a 20.7 % reduction in *SCE* during the face milling of steel [70], and an archive-based micro-genetic algorithm had also been used to identify optimal solutions for reducing *SCE* and improving surface finish [44].

In an experimental study *GRA* had been employed to optimize various aspects of machining, including the cost of cutting tool components, energy utilization, tool wear, and surface finish [71]. For different machining conditions such as minimum quantity lubrication, dry, and flooded, bacteria foraging optimisation and particle swarm optimisation have been utilized to optimize V_c, *ap*, and f_z with the aim of minimising tool wear [72]. Meanwhile, an analytical hierarchy approach and *GRA* showed that the interaction of cutting conditions has a greater effect on machining responses than individual parameters when machining difficult-to-cut alloys such as titanium [73]. Wet machining was found to deliver superior tool wear and surface quality compared to dry machining, although the latter yielded lower *SCE* due to thermal softening at higher temperatures. Cryogenic conditions are also useful for achieving preferable response parameters [74,75].

This research aims to optimize *SCE*, R_a, and burr size by varying V_c, *ap*, *Z*, and f_z. To this end, a multi-objective function was being formulated with a focus on input parameters that have not yet been optimised. In addition, burr formation in macro-milling and the impact of the *Z* on responses has not been broadly reported in the literature. A trade-off between machining parameters and responses was established through multi-objective optimisation (*MOO*) utilizing *GRA* within this experimental study.

2. Research motivation

This research aims to optimize multiple response factors during milling operations, including R_a, *SCE*, and burr width on up ($B_{w\ up\ milling}$) and down milling ($B_{w\ down\ milling}$) sides of the workpiece. Sustainable machining can be achieved through this process, along with improved surface quality and dimensional accuracy, allowing to produce finished or near-finished parts with minimal deburring needs. However, research on burr formation in macro-milling is limited and the influence of the *Z* on R_a and *SCE* has not been extensively published to the best of author's knowledge. It is evident that the identification of optimal machining parameters is crucial in achieving efficient and sustainable machining processes while maintaining high-quality surface finishes.

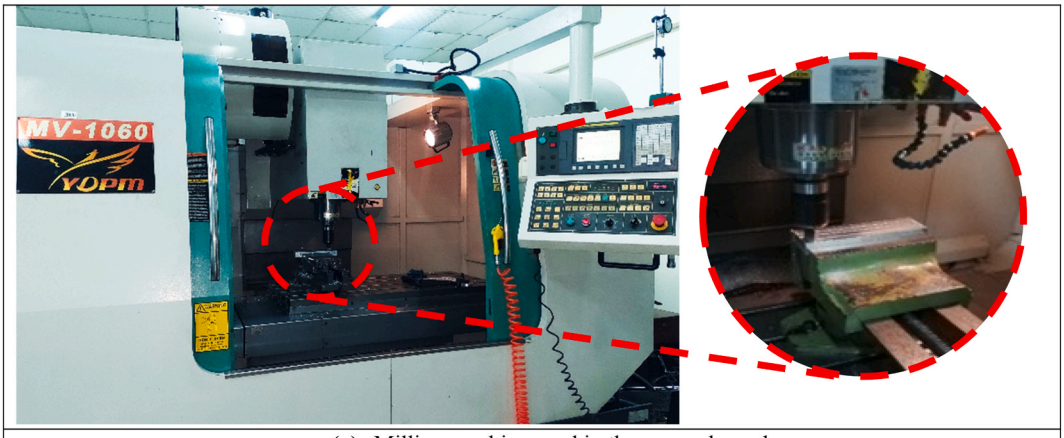

(a) Milling machine used in the research work

(b) Metallurgical microscope used in this study.

(c) Roughness tester used in this study.

(d) Yokogawa Cw240 power analyser

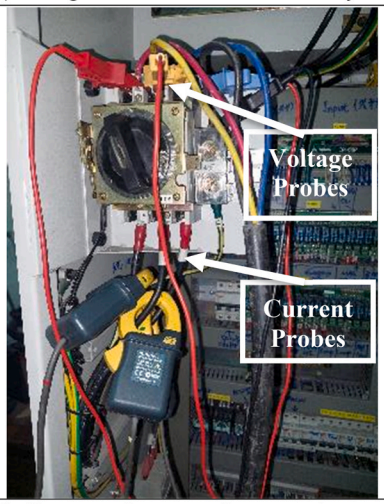

(e) Power analyzer attachment to the machine

Fig. 1. Experimental setup (a) Milling machine MV-1060 YDPM, (b) MT8530 optical microscope, MEIJI Techno Co., Saitama, Japan, LTD, (c) Roughness tester TIME ® 3110, (d) Yokogawa Cw240 power analyser, and (e) Power analyzer attachment to the machine.

3. Materials and methods

The details of material, apparatus, responses recorded in this study, and design of experiment used in this study are described in detail in the subsequent parts.

Table 1
Chemical composition of aluminium 6061-T6 (adopted from Ref. [90]).

	Al	Mg	Si	Cu	Fe	Cr	Mn	Zn	Ti
%	~Bal	1.1	0.62	0.29	0.22	0.18	0.07	0.01	0.01

Table 2
Mechanical properties of aluminium 6061-T6 (adopted from Ref. [90]).

Hardness (HV)	Yield Strength (MPa)	Tensile Strength (MPa)	Elongation %
101–108	250–260	280–300	12.0–14.0

3.1. Experimental material

This research utilized the YDPM MV 1060 milling machine from YIDA Precision Machinery (shown in Fig. 1), Taiwan, featuring a table dimension of 1180 × 540 mm and a working area of 1060 × 620 mm, with a maximum load capacity of 1000 kg. The cutting tools included two 25 mm diameter variants: R390-025B25-11 M, accommodating three inserts at 120-degree intervals, and R390-025B25-11L, capable of mounting two inserts at 180-degree intervals. The inserts, R390-11 T3 02E-KM H13A from Sankvik, featured a 90-degree principal edge angle, effective cutting-edge length of 10 mm, and a nose radius of 0.2 mm. The maximum admissible V_c of the insert was 1000 m/min, and the recommended f_z range by the manufacturer was 0.08–0.18mm/tooth. According to published literature, tool wears due to the machining parameters [76] and this can affect energy consumption [77,78]. To prevent the repercussions of tool wear on energy expenditure, a fresh insert was used for each machining condition. The tool holder used was WALTER A170 M.063.080.25. These precision tools and inserts facilitated the exploration across various cutting scenarios, adhering strictly to manufacturer-prescribed machining parameters.

Aluminium Al 6061-T6, which is among the most abundant element on earth [79] and commonly utilized in architecture, transportation, and food industry [80,81], was selected as the workpiece material. Notably, the aerospace industry often employs aluminium due to its impressive strength-to-weight ratio as well [82]. The chosen material for this study, aluminium Al 6061-T6, was selected with the aim of improving surface quality and reducing energy consumption during machining of this commonly used material. Table 1 illustrates the chemical composition of Al 6061-T6 and Table 2 shows its mechanical properties.

During machining, the phenomenon of aluminum adhering to the cutting insert, commonly known as built-up edge (BUE), poses a significant challenge [83,84]. This adherence results in tool blunting and increased energy consumption [71,85]. This issue was effectively mitigated by employing a fresh insert for each slot. Furthermore, specific cutting energy was precisely measured, with time tracking conducted in accordance with previous studies [34,86]. Additionally, burr width was meticulously measured through thorough microscopic examination, with the largest burr on any side of the slot considered a response variable, as per established methodology [87–89]. These challenges, inherent to machining processes, were successfully addressed, ensuring accurate measurement and analysis in this study.

3.2. Machining responses

The experiment aimed to investigate R_a, *SCE*, and burr width on the up-milling (B_w *up-milling*) and down-milling (B_w *down-milling*) side of the workpiece as response parameters. The aluminium block, measuring 20 mm thick, 200 mm wide, and 400 mm long, served as the substrate for milling operations and subsequent measurements of surface roughness and burr width. Surface roughness assessment was conducted using the Times® 100 surface roughness tester (Fig. 1 (c)), featuring an RC analogue filter, 6 mm tracing length, and 1 mm/s scan speed. Prior to each measurement, meticulous cleaning of the slot was ensured through air pressure and alcohol. Ra measurements were taken at three points along each slot—beginning, middle, and end—and repeated thrice for accuracy. Burr width examination utilized the MEIJI Techno Co., LTD MT8530 metallurgical microscope (Fig. 1 (b)), equipped with an infinity corrected optical system with F-200 mm, an infinity tube lens with 200 mm focal length, and a vertical Köhler illuminator with a 12V 50W halogen lamp, enabling measurements on both sides.

Power consumption was monitored with the YOKOGAWA Model CW240 three-phase power analyser (Fig. 1 (d) and I (e)), capable of measurements at intervals of 0.1 s, connected to the machine's power supply via current and voltage probes. *SCE* was calculated by dividing power consumption during cutting over *MOO* as already done by past researchers [34,91]. Equations (1) and (2) are used in calculating SCE.

$$SCE = \frac{P_{cut}}{Material\ removal\ rate\ (V\ x\ F\ x\ D)} \tag{1}$$

Where, $P_{cut} = P_{actual} - P_{air}$ (2)

In the equations (1) and (2), P_{air} is the amount of power consumed during air cut when no material is being removed from the workpiece and there is no interaction between the workpiece and tool. However, the machine tool follows the programmed machining parameters. P_{actual} is the total amount of power consumption during actual cut, which includes power consumption in the whole

Table 3
Machining parameters and their levels used in this study.

Levels	*ap* (mm)	V_c (m/min)	f_z (mm/tooth)	*Z*
1	1.0	100	0.10	1
2	1.5	225	0.14	2
3	2.0	350	0.18	3

Table 4
Taguchi L9 orthogonal array along with their measured responses.

Exp #	*ap* (mm)	V_c (m/min)	f_z (mm/tooth)	*Z*	*SCE* (J/cm^3)	R_a (μm)	B_w *up-milling* (μm)	B_w *down-milling* (μm)
1	1	100	0.1	1	1548.95	0.1316	329.6	331.6
2	1	225	0.14	2	1241.52	0.1625	201.0	341.0
3	1	350	0.18	3	1133.20	0.2733	177.6	308.3
4	1.5	100	0.14	3	1307.29	0.2025	230.6	278.3
5	1.5	225	0.18	1	1126.89	0.1158	268.1	313.3
6	1.5	350	0.1	2	1224.39	0.1241	183.3	262.0
7	2	100	0.18	2	1264.06	0.1158	179.6	281.0
8	2	225	0.1	3	1195.62	0.1883	233.7	445.0
9	2	350	0.14	1	1121.11	0.1208	181.0	232.6

machining process. P_{cut} is the difference between total power consumption during material removal and power consumption during air cut. In other words, P_{cut} can be regarded as actual power required for material removal only. It is pertinent to mention that total power consumption during machining is dependent on machine tool. Larger sized machines may consume greater amount of total power during material removal process while smaller sized machines may consume lesser amount of power. It is because about 14.8 % of the total energy during any machining process is consumed in material removal, remaining all the energy is consumed by other components of the machine, like coolant flow, oil pressure pump cooler mist collector etc [92]. It has already been established that *SCE* is independent of machine tool [86] and hence *SCE* is used in this research as well.

3.3. Experiment design

In this research work *ap*, V_c, f_z and *Z* were varied in 3 levels. The selection of varied machining parameters as variables in the study reflects their common variability in practical machining settings. The focus on these parameters is justified by their practical and frequent adjustments on the shop floor. Parameters including spindle speed and material removal rate are derived from these variables. Furthermore, all four machining parameters chosen as variables have been widely recognized in the literature as key influencers of the measured responses in the study, as evidenced by literature [45,68,89,93].

The experimental plan is presented in Table 3 f_z and *ap* are within the recommended range of manufacturer of end mill cutter and inserts [94]. Taguchi L9 array (developed by Genichi Taguchi [95]) was employed for experiment design. This technique is reported to be one of the most efficient way to reduce number of experiments without compromising the results [96,97]. Each experiment was repeated thrice to minimize any errors in the results and mean value of the responses were used for analysis and calculations.

Main effect plots of each measured machining responses are individually analysed first, and then for optimisation, grey relation analysis is employed to calculate the grey relation grade against each machining parameter. Grey relation grade *(GRG)* was obtained using equal weightage approach. Lastly, optimised model is validated for the obtained results.

4. Results and discussion

The results are categorized in two parts. First is the statistical analysis including main effects plot and analysis of variance. In the second step, multi objective optimisation is carried out using grey relational analysis.

4.1. Analysis of response parameters

The complete design of experiment along with the recorded responses is presented in Table 4.

The effect of cutting parameters on the response parameters are expressed in the graphs as shown in Fig. 2. The recorded responses are plotted against each input parameter in the same graph for a comparative view. Each input was individually analysed.

4.1.1. Effect of feed per tooth

As depicted in Fig. 2 (a), it is observed that there is an increase in R_a with the increase in f_z, which results in a compromise in surface finish. However, the increase in f_z leads to a decrease in *SCE* and B_w *down-milling*. A similar trend of R_a concerning f_z was also reported in previous studies during the milling of aluminium Al 6061-T6 [98]. However, V_c was varied in a very short range (i.e. 275 m/min to 325 m/min) in the said research. R_a increases as the chip volume increase, which in turn depends on increase in f_z and *Z* [99]. Additionally increase in f_z also increases the cutting forces which compromises the surface quality [58]. The *SCE* reduces as the f_z was

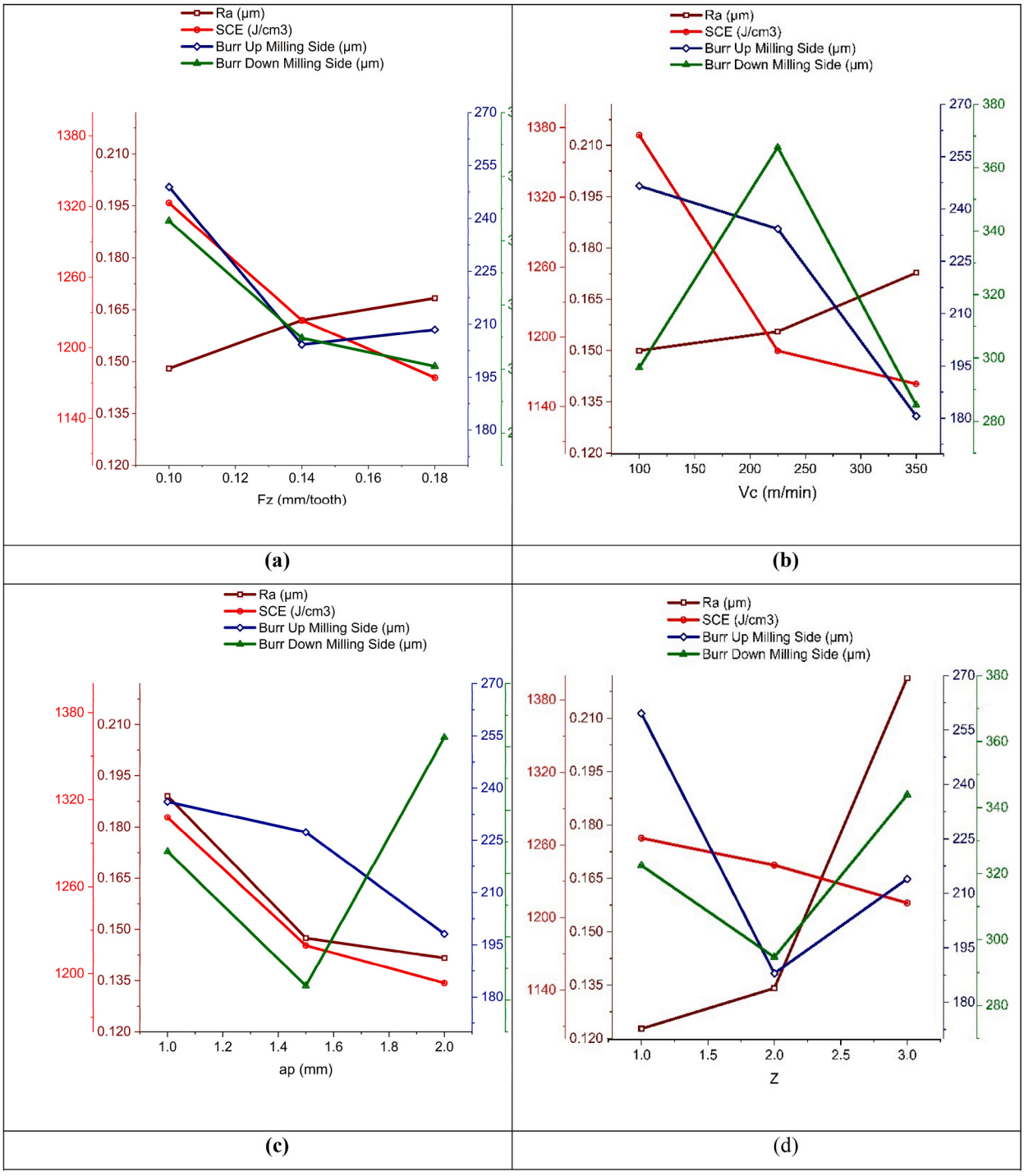

Fig. 2. Main effect plots of response parameters (a) effect of f_z, (b) V_c, (c) *ap*, (d) *Z*.

increased. This is because the increase in f_z also increases the *MRR*. Keeping in view equation (1), increase in *MRR* leads to lower value of *SCE*. Furthermore, increase in f_z leads to sudden decrease in B_w *up-milling* and then slight increase in the said response.

4.1.2. Effect of cutting speed

Fig. 2 (b) demonstrate that R_a increased as V_c was increased over three intervals. However, *SCE* and burr width decreased on the up-milling side. On the down-milling side, burr width initially increased and then decreased with an increase in V_c. These results can be

Table 5
Identified machining parameters for best and worst response.

Input Parameters	Responses							
	Ra (μm)		*SCE* (J/cm^3)		$B_{w\ Up\text{-}Milling\ side}$ (μm)		$B_{W\ Up\text{-}Milling\ side}$ (μm)	
	Best	Worst	Best	Worst	Best	Worst	Best	Worst
F_z (mm/tooth)	0.1	0.18	0.18	0.1	0.14	0.1	0.14	0.1
V_c (m/min)	100	350	350	100	350	100	350	225
ap (mm)	2	1	2	1	2	1	1.5	1
Z	1	3	3	1	2	1	1	3

attributed to a higher chip volume resulting in increased R_a and an increase in temperature due to higher V_c [100]. Compared to steel and other ferrous metals, aluminium has a lower melting point, resulting in faster material smearing with inserts during low-speed machining. This leads to a build-up of edge and increased R_a. Studies have already reported a similar pattern of R_a on steel [101, 102]. Increasing the V_c amplifies the amount of cutting forces [103] and higher cutting forces are a contributing factor for increased R_a. Furthermore, an increase in V_c also leads to an increase in the vibration amplitude, resulting in higher R_a [104]. It is noteworthy that the surface finish can be improved during high-speed machining by increasing the V_c, while the surface quality can deteriorate in low or conventional speed ranges due to the formation of build-up edge (especially in metals with lower melting points). This is because increasing V_c reduces the time that the tool spends in contact with the workpiece, minimising the heat generated and the material deformation, which leads to a smoother surface. Specific cutting energy consumption is the key factor for industry [105], and there is an inverse relationship between *SCE* and R_a.

Increase in V_c improves surface finish during high-speed machining, though this isn't the case for low speed or conventional machining where build-up edge is formed [106] and there is an inverse relation between Specific Cutting Energy Consumption and R_a. Higher V_c have been found to lead to decreased specific cutting energy consumption through thermal softening and change of friction coefficient [107]. Burr width on the up-milling side decreases as V_c increases, but on the down milling side there can either be an increase or decrease with increased speed [89,108,109]. Published literature reveals that the relation between burr width and machining parameters is inconsistent, as burr width undergoes dramatic changes with the alteration of workpiece or tool material, as well as other machining parameters.

4.1.3. Effect of depth of cut

Considering Fig. 2 (c) R_a, specific cutting energy, and burr width on up-mill side is observed to reduce with the increase in *ap*. During the experiment, B_w *down-milling* side decreased in size before increasing with the deepening *ap*. It is important to note that the *ap* is the only machining parameter which affects both the *SCE* and the R_a in an identical way. Increasing the *ap* resulted in a decrease in *SCE* and cutting forces, leading to a better surface finish in this experiment [76]. Low cutting forces meant less elastoplastic deformation, resulting in an improved surface quality [85]. As process parameters increased, so did temperature which resulted in a softer material and lower specific cutting energy [10,31,44]. When machining ductile materials, a higher *ap* produces lower tensile stress on the chips that are about to detach from the work piece, resulting in the production of smaller burrs at deeper *ap* [110]. A rise in *ap* also contributes to larger burrs and higher cutting forces, which are both contributing in larger burr size [58].

4.1.4. Effect of number of inserts

Main effect plots shown in Fig. 2 (d) depicts that lesser *Z* leads to better surface finish and lesser B_w *down-milling* side in contrast to specific cutting energy for which using greater *Z* lowers specific cutting energy consumption. However, in case of burr width on up-milling side maximum burr width is noted when one insert was used, then there is a decrease in burr width when two inserts were used and then subsequently burr width again surges when three inserts were used. The effect of *Z* on response parameters used in this study has not been extensively reported in the literature. *Z* are reported to be one of the significant machining parameter in affecting R_a, and surface quality can be increased by reducing *Z* during milling [111]. It has been published in the literature that adding more inserts and cutting edges while machining titanium alloy, increases the number of passes [99] and vibrations on the workpiece, leading to an higher R_a [112]. When machining parameters are set to higher values, the machining efficiency is improved, and *SCE* is reduced [113]. The ploughing effect is more noticeable at a higher *Z* and V_c, resulting in larger burr sizes [52,110].

It is essential to emphasize that the limited literature available on burr formation during macro milling suggests that there is no consistent behaviour in forecasting burr size [60,64,89,114]. Previous studies have found similar findings of larger burrs on the down milling side [57,93,115], which can be attributed to the fact that materials tend to deform in the direction of the force, leading to smaller burrs [63]. Additionally, higher velocities of localized cutting edges also produce smaller burrs.

4.1.5. Validation of best and worst machining parameters based on main effect plots

In this study the machining responses, R_a, *SCE*, $B_{w\ down\text{-}milling}$ and $B_{w\ Up\ milling}$ are based on smaller the better model. Best and worst machining conditions were noted from Fig. 2 and presented in Table 5.

Best surface finish was noted at minimum f_z, V_c, *Z* and maximum *ap*. Lowest *SCE* was recorded at highest values of machining parameters. Lowest burr width was noted on intermediate level of f_z and *ap*, along with minimum V_c and least *Z*. Least $B_{w\ Up\ milling}$ was recorded at intermediate level of f_z and using 2 inserts along with maximum V_c and *ap*.

Table 6
Grey relation coefficient for each measure machining response, grey relation grade and rank of each machining parameter.

Machining Parameters					Grey Relation Coefficients				*GRG*	Rank
Exp. No.	f_z *(mm/tooth)*	V_c *(m/min)*	*ap (mm)*	*Z*	R_a	*SCE*	$B_{wUp\ milling}$	$B_{wDown\ milling}$		
1	0.1	100	1	1	0.83	0.33	0.33	0.51	0.507	9
2	0.14	225	1	2	0.62	0.63	0.76	0.49	0.631	6
3	0.18	350	1	3	0.33	0.94	1	0.58	0.688	5
4	0.14	100	1.5	3	0.47	0.53	0.58	0.69	0.567	7
5	0.18	225	1.5	1	1	0.97	0.45	0.56	0.730	4
6	0.1	350	1.5	2	0.90	0.67	0.93	0.78	0.803	2
7	0.18	100	2	2	0.99	0.59	0.97	0.68	0.785	3
8	0.1	225	2	3	0.52	0.74	0.57	0.33	0.532	8
9	0.14	350	2	1	0.94	1	0.95	1	0.936	1

4.2. Grey relation analysis for multi objective optimisation

In machining process, the response variables like R_a, burr size, energy consumption and tool wear depend on the machining parameters. Obtaining the lowest levels of surface finish, specific cutting energy, and burr width at the same time does not seems to be realistic. For instance, the main effect plot in Fig. 2 shows that decreasing f_z and number of cutting inserts will lead to better surface finish but at the same time will also lead to higher energy consumption and larger burr width. So, *MOO* is very helpful to set a trade-off between machining responses and to determine most optimised machining parameters.

4.2.1. Need for multi objective optimisation

Grey relation analysis is employed for optimisation of machining parameters, which is also used by previous researchers for optimisation of machining parameters [4,73,116]. Grey relation analysis based on Taguchi design of experiment produces a grey relation grade which is a single unique function. This single unique function helps in establishing the rank of machining parameters and can determine the order or hierarchy of optimised combinations of machining parameters [117,118]. RSM was preferred over other techniques like ANN for optimisation due to its established systematic approach [119–122] and interpretability in understanding the relationship between process variables and responses, aligning with the study's specific needs and constraints. Keeping in view the published literature some necessary steps performed for grey relation analysis are described below [4,73,123].

4.2.2. Data processing

The first step in grey relation analysis is normalizing all the machining responses on a scale of 0–1. This step is objective based and is performed keeping in view the desired outcome of machining responses. For instance, the objective during normalization of some of the machining responses like R_a, burr size, energy consumption and tool wear should be smaller the better. However, the objective during normalization of machining responses like *MOO* should be higher the better. In this research the aim is to minimize the recorded machining responses (R_a, *SCE*, burr size) hence equation (3) is used for normalization [123].

$$Zij = \frac{\max\,(yij, i = 1, 2, \ldots..n) - yij}{\max\,(yij, i = 1, 2, \ldots.n) - \min\,(yij, i = 1, 2, \ldots.n)} \tag{3}$$

Here j = 1, 2, …m and i = 1, 2, …n where m is the number of responses studied and index n is the count of experimental data parameters.

4.2.3. Grey relation coefficient (GRC) calculation

After normalization of the values on a scale of 0–1, grey relation coefficients are calculated using equation (4) [4,124].

$$\gamma(Z_0, Zij) = \frac{\Delta min + \xi \Delta max}{\Delta_{oj}(k) + \xi \Delta max} \tag{4}$$

Here the value of γ (Z_o, Z_{ij}) is less than or equal to 1 but greater than 0. $Z_{ij}(k)$ and $Z_o(k)$ are the comparability and reference sequences, respectively, where $Z_o(k) = 1$, k = 1 … m. Equation (5) is used to calculate the deviation sequence [4,70].

$$\Delta_{oj}(k) = \left|Z_o(k) - Z_{ij}(k)\right| \tag{5}$$

Δmax and Δmin corresponds to the largest and smallest values of Δ_{oj} (k). The distinguishing coefficient ξ is kept equal to 0.5 if all parameters have same weightage, otherwise the distinguishing coefficient ranges between 0 and 1 depending upon the weightage of machining parameters. The Grey relation coefficient for each measured response, grade and rank of each experiment is presented in Table 6.

4.2.4. Grey relation grade (GRG) calculation

The varying multiple objectives, in this step are converted to single grey relation grade *(GRG)*. By maximizing the *GRG*, optimum results can be attained. Equation (6) is used to calculate the *GRG* [73].

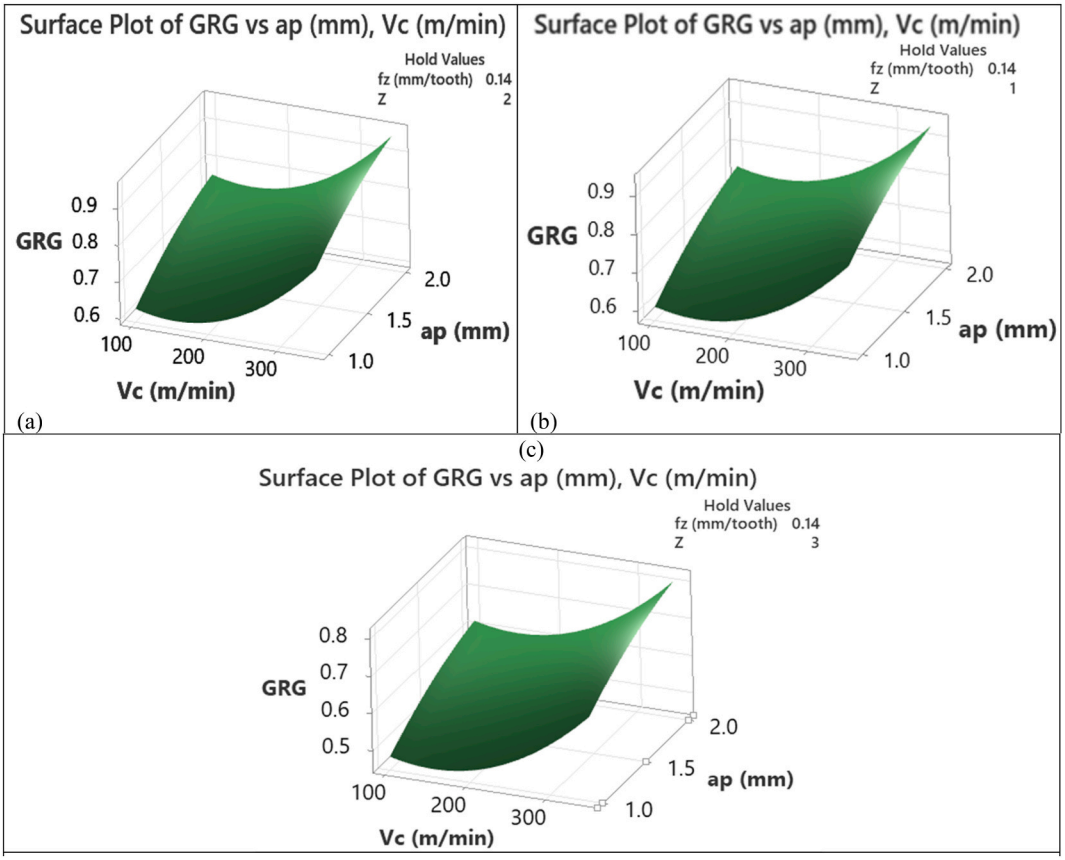

Fig. 3. Surface plots of *GRG* vs machining parameters (a) $Z = 1$ (b) $Z = 2$ (c) $Z = 3$.

$$\text{Grade}\,(Z_0, Zij) = \sum_{r=1}^{n} \omega_r \gamma\left(Z_0, Z_{ij}\right) \tag{6}$$

Where ω_r is the weight of rth objective. Usually, weight is assigned by prescribed policy or customers requirement. For instance, if the customer requirement is finished or near finished part and energy consumption is not the point of interest then the weightage for burr size and R_a may be kept greater than the weightage assigned to *SCE*. However, in this research equal weightage is assigned to all the machining parameters. This approach of equal weightage is used by previous researchers as well [125–127]. The equation (6) can be transformed to equation (7) after assigning equal weightage.

$$GRG = 0.25GRC_{SCE} + 0.25GRC_{Ra} + 0.25GRC_{Bw\ upmill} + 0.25GRC_{Bw\ downmill} \tag{7}$$

Where GRC_{SCE}, GRC_{Ra}, $GRC_{Bw\ upmill}$, and $GRC_{Bw\ downmill}$ corresponds to grey relation coefficient of specific cutting energy, grey relation coefficient of average R_a, grey relation coefficient of $B_{w\ Up\ milling}$ and grey relation coefficient of $B_{\text{w down-milling}}$ side respectively.

Experiment 9, with parameters of ($V_c = 350$ m/min, $f_z = 0.14$mm/tooth, $Z = 1$, and $ap = 2$ mm) and a Rank of 1, had the highest Grey Relation Grade value according to Table 6. Least grey relation grade was observed for experiment 1 corresponding to parameters ($f_z = 0.1$mm/tooth, $V_c = 100$ m/min, $ap = 1$ mm and $Z = 1$) and rank 9. Using Table 6 regression equations were obtained by employing response surface analysis.

4.3. Regression modelling of multi objective function

A comprehensive regression analysis was carried out which comprises regression analysis and optimisation as well. Through ANOVA, the significance and contribution rate of each machining parameter was evaluated. Then confirmatory experiments were conducted twice for the most optimised machining parameters for validation. Step wise regression analysis, analysis of variance and optimisation is discussed in detail below.

Response surface method was employed for optimisation of regression model. In this research 3 machining parameters (V_c, ap and f_z) were considered as continuous predictors and Z was considered as categorical predictor. Three separate functions each of $Z = 1$, 2 and 3 were obtained. These equations are shown in equation (8), equation (9) and equation (10) for $Z = 1$, 2, and 3 respectively.

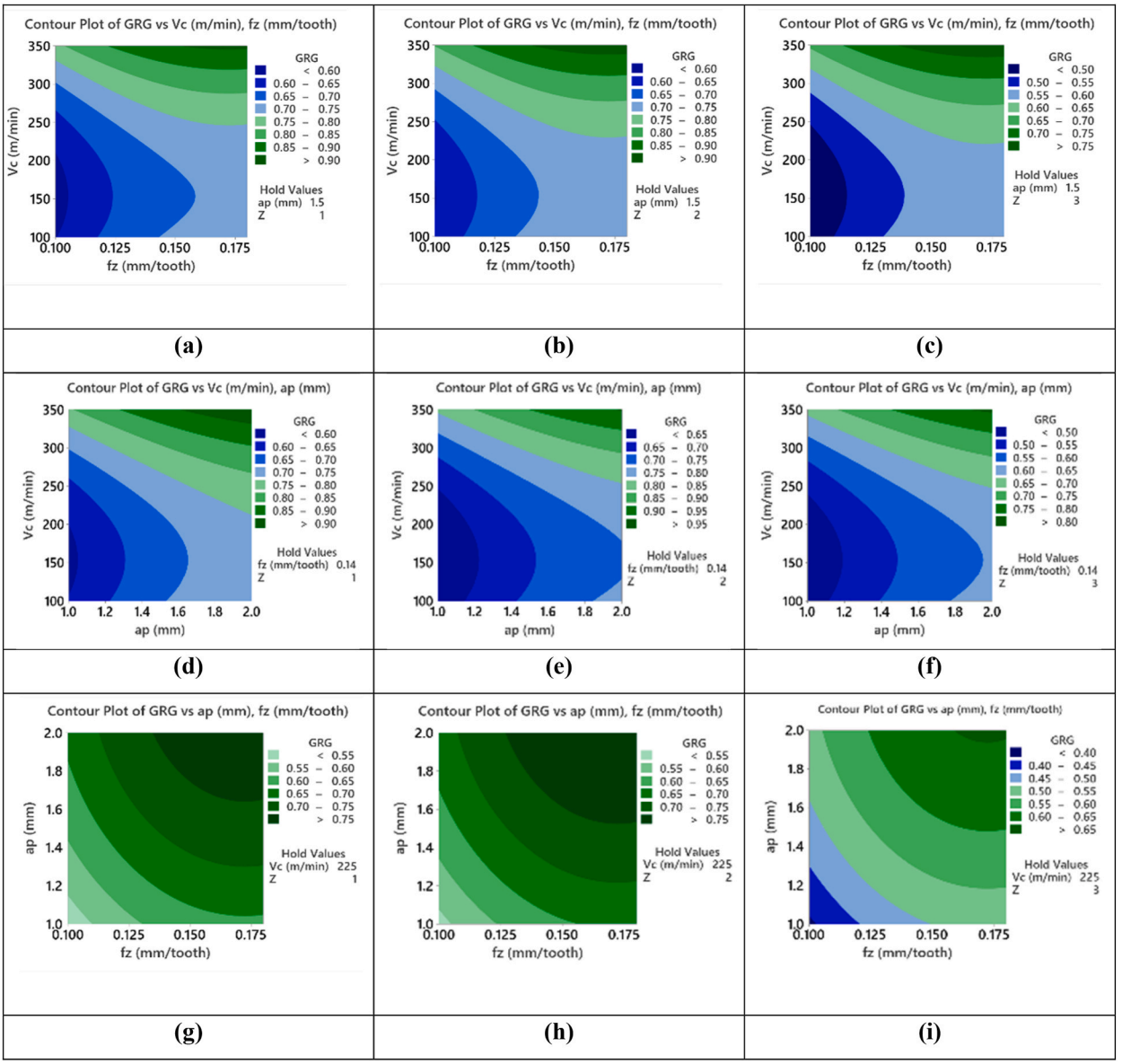

Fig. 4. Contour plots of machining responses VS *GRG* (a) V_c Vs f_z at $Z = 1$, (b) V_c Vs f_z at $Z = 2$, (c) V_c Vs f_z at $Z = 3$, (d) V_c Vs ap at $Z = 1$, (e) V_c Vs ap at $Z = 2$, (f) V_c Vs ap at $Z = 3$, (g) ap, V_c, f_z at $Z = 1$, (h) V_c Vs f_z at $Z = 2$, and (i) V_c Vs f_z at $Z = 3$.

$$GRG\left(f_z, V_c, d, Z\right) = -0.252 + 8.03f_z - 0.001643V_c + 0.379d - 23.3f_z * f_z + 0.000005V_c * V_c - 0.0789d * d \quad (8)$$

$$GRG\left(fz, Vc, d, Z\right) = -0.237 + 8.03fz - 0.001643Vc + 0.379d - 23.3fz * fz + 0.000005Vc * Vc - 0.0789d * d \quad (9)$$

$$GRG\left(fz, Vc, d, Z\right) = -0.381 + 8.03fz - 0.001643Vc + 0.379d - 23.3fz * fz + 0.000005Vc * Vc - 0.0789d * d \quad (10)$$

Fig. 3 (a), (b), and (c) shows the surface plots of GRG corresponding to machining parameters when $Z = 1$, 2 and 3 respectively, while holding the value of f_z at 0.14mm/tooth. It can be observed from the graphs that maximum values of ap and V_c while using any Z yields highest GRG.

Contour plots of machining responses corresponding to *GRG* are shown in Fig. 4 (a) to (i). Each plot depicts the achievable highest and lowest *GRG* against 2 machining parameters while holding the other two machining parameters at fixed values.

4.3.1. Analysis of variance

Table 7 displays the ANOVA results of the regression analysis. It can be observed that V_c has the highest contribution ratio, followed by the Z, ap, and f_z. Furthermore, all of the machining parameters utilized in this experimental study are significant based on their

Table 7
ANOVA test on GRG.

Analysis of Variance							
Source	DF	Seq SS	Contribution	Adj SS	Adj MS	F-Value	P-Value
Regression	5	0.43041	82.62 %	0.43041	0.086081	19.97	0
f_z (mm/tooth)	1	0.0652	12.52 %	0.0652	0.0652	15.13	0.001
V_c (m/min)	1	0.16183	31.07 %	0.16183	0.161831	37.55	0
ap (mm)	1	0.09134	17.54 %	0.09134	0.091344	21.19	0
Z	2	0.11203	21.51 %	0.11203	0.056015	13	0
Error	21	0.09051	17.38 %	0.09051	0.00431		
Lack-of-Fit	3	0.05242	10.06 %	0.05242	0.017472	8.25	0.001
Pure Error	18	0.0381	7.31 %	0.0381	0.002117		
Total	26	0.52092	100.00 %				

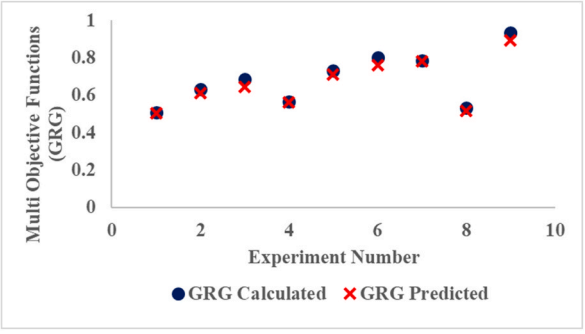

Fig. 5. Comparison between Calculated *GRG* from regression model and *GRG* obtained experimentally.

Table 8
Optimisation comparison between the best experimental run and the optimised run.

	Machining Conditions				Responses			
	V_c	F_z	ap	Z	R_a	SCE	$B_{w\ Up\ milling}$	$B_{w\ down\text{-}milling}$
Best Run	350	0.1400	2	1	0.1208	1121.11	181.0	232.6
Optimised Run	350	0.1725	2	2	0.0946	993.42	197.3	218.0

respective P-values.

4.3.2. Regression model optimisation

Suitable machining parameters for optimised responses or outputs were computed using response surface method. The optimised regression model with maximum achievable grey relation grade was also experimentally validated and the result is presented in Fig. 4. Fig. 5 shows the comparison between calculated *GRG* from regression model and *GRG* obtained experimentally. It is evident from the figure that the predicted *GRG* from the equations (8)–(10) is very close to the *GRG* calculated.

4.3.3. Validation experiments

The machining parameters that were optimised through *RSM* and the best run conditions of the initial experiments (experiment #9) are shown in Table 8. Upon validation, these conditions revealed a considerable improvement in the results. R_a, *SCE*, and $B_{w\ down\text{-}milling}$ were reduced by 21.69 %, 11.39 %, and 6.2 % respectively, while $B_{w\ Up\ milling}$ was increased by 9 %.

Fig. 6 shows the surface optimisation of *GRG*. The optimised values of machining parameters can be observed from the figure i.e., f_z = 0.1725mm/tooth, V_c = 350 m/min, ap = 2 mm, and Z = 2. These values of machining parameters were used in experimental validation of optimised results. The burr width found on up and down milling side of the optimised machine parameters is presented in Fig. 7 (a) and (b) respectively.

Such an analysis of optimised machining parameters allows for an efficient and sustainable approach to manufacturing, while providing an opportunity to minimize energy costs and produce near-finished parts with minimal deburring requirements.

5. Conclusion

The present research focused on optimisation of machining responses under varying machining conditions. *GRA* was used for optimisation. The experimental results showed interesting conclusions and leads towards better production rates along with

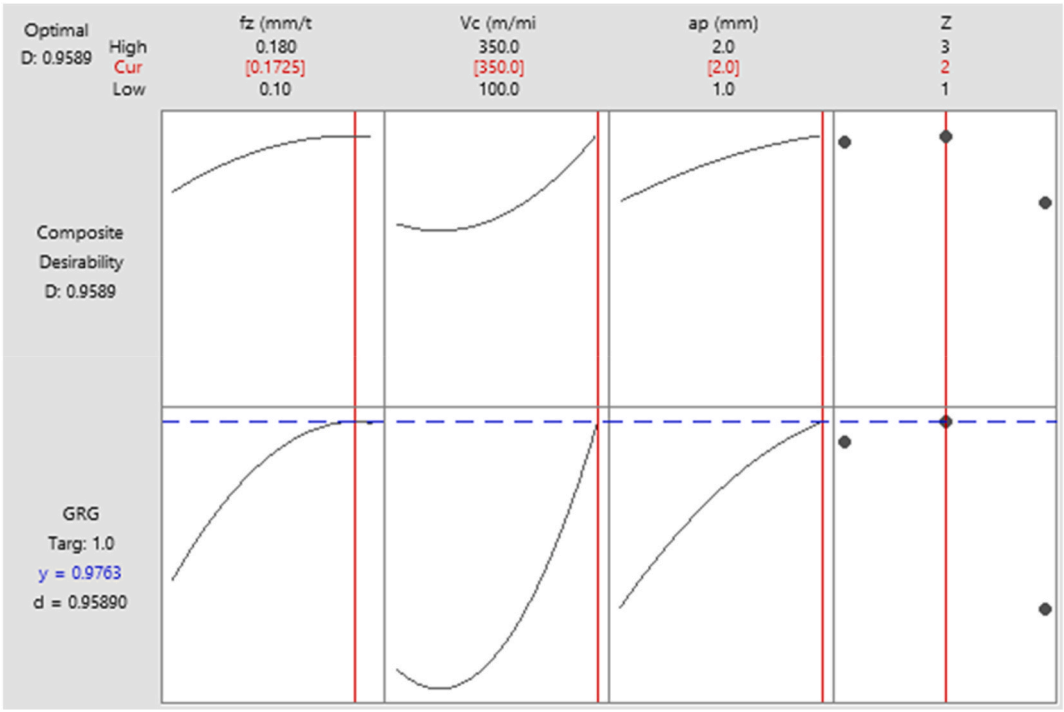

Fig. 6. GRG response surface optimisation.

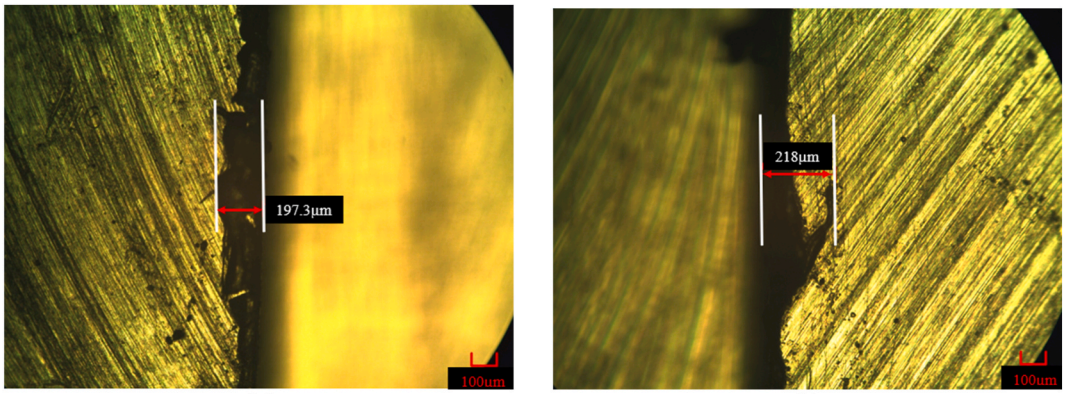

(a) **(b)**

Fig. 7. **(a)** $B_{w\ Up\ milling}$ noted during optimised run, **(b)** $B_{w\ down\text{-}milling}$ noted during optimised run.

improvement in surface quality and leads towards sustainable machining in terms of *SCE*. Few prominent conclusions that can be drawn from the present research are discussed below.

1. f_z is identified as a vital machining input decreasing *SCE* at higher f_z values improving process sustainability as well as reducing B_w *down-milling* side. On the contrary, higher R_a is resulted at higher f_z values.
2. *SCE* and $B_{w\ Up\ milling}$ were found to improve in elevated V_c region. Surface integrity was adversely affected at V_c values.
3. *ap* is observed as the only machining parameter having identical effects on R_a, *SCE* and $B_{w\ Up\ milling}$ i.e., increase in *ap* reduces these responses.
4. Best surface finish was observed while using one cutting insert, whereas minimum *SCE* was observed while using three inserts. Increasing *Z* reduces the *SCE* however, it compromises the surface finish due to ploughing effect and increasing number of passes on the workpiece.
5. Machining conditions of 0.14 mm/tooth f_z, 350 m/min V_c and 2 mm *ap* using 1 cutting insert (exp no 9) was identified as the best machining run using grey relational analysis owing to its highest grey relational grade of 0.936.

6. Analysis of variance results revealed that V_c has the major effect on grey relational grade having a contribution ratio of 31.07 %, followed by Z (21.51 %), ap (17.54 %) and f_z (12.52 %).
7. Regression modelling of formulated grey relational grades functions (separate for each no of inserts) highlighted function of 3 cutting inserts to have a positive intercept gain of 50 % and 60 % as compared to the 1 and 2 cutting insert functions, respectively.
8. Validation of optimised machining parameters, identified using response surface methodology, significantly improved the surface quality while reducing energy consumption. It was revealed that using the optimised machining parameters improved surface finish by 21.7 %, SCE by 11.39 % and $B_{w\ down\text{-}milling}$ by 6.2 %. However, $B_{w\ Up\ milling}$ was increased by 9 %.
9. Based on this experimental study it can be concluded that machining responses can be improved, predicted and optimised. However, the response of burr width is observed to be inconsistent and non-predictable. The only consistent observation regarding burr width is observed to be smaller $B_{w\ Up\ milling}$ as compared to $B_{w\ down\text{-}milling}$.
10. In this experimental study, it is also concluded that achieving sustainability in energy and economy is feasible through the implementation of appropriate machining parameters. However, it's crucial to acknowledge that not all four measured responses may meet desired levels. Nevertheless, employing optimisation techniques can offer a solution by enabling a trade-off among machining parameters. By utilizing optimised machining parameters, manufacturing industries can reduce costs and contribute to sustainable manufacturing practices. This approach also provides a competitive advantage in terms of production rate, surface quality, and energy efficiency.

Funding

This article was co-funded by the European Union under the REFRESH – Research Excellence For Region Sustainability and High-tech Industries project number CZ.10.03.01/00/22_003/0000048 via the Operational Programme Just Transition. This work was supported by the Deanship of Scientific Research, Vice Presidency for Graduate Studies and Scientific Research, King Faisal University, Saudi Arabia (Grant No. KFU241300).

CRediT authorship contribution statement

Sajid Raza Zaidi: Conceptualization, Data curation, Formal analysis, Investigation, Validation, Writing – original draft. **Shahid Ikramullah Butt:** Conceptualization, Investigation, Methodology, Resources, Supervision, Visualization. **Muhammad Ali Khan:** Conceptualization, Data curation, Formal analysis, Funding acquisition, Resources, Software, Supervision, Validation, Visualization, Writing – original draft. **Muhammad Iftikhar Faraz:** Conceptualization, Formal analysis, Investigation, Project administration, Software. **Syed Husain Imran Jaffery:** Formal analysis, Funding acquisition, Investigation, Methodology, Supervision, Visualization, Writing – original draft. **Jana Petru:** Data curation, Investigation, Methodology, Resources, Software, Validation, Visualization.

.Declaration of competing interest

The authors declare that they have no known competing financial interests or personal relationships that could have appeared to influence the work reported in this paper.

References

[1] M.P. Groover, Fundamental of Modern Manufacturing Material, Processes, and System, fifth ed., 2012.
[2] M.C. Shaw, METAL CUTTING PRINCIPLES, second ed., Oxford University Press, June, 2001.
[3] Y. Guo, L. Wang, Z. Zhang, J. Cao, X. Xia, Y. Liu, Integrated modeling for retired mechanical product genes in remanufacturing: a knowledge graph-based approach, Adv. Eng. Inf. 59 (Jan. 2024) 102254, https://doi.org/10.1016/J.AEI.2023.102254.
[4] M.A.M. Khan, et al., Multi-objective optimization of turning titanium-based alloy Ti-6Al-4V under dry, wet, and cryogenic conditions using gray relational analysis (GRA), Int. J. Adv. Manuf. Technol. 106 (9–10) (2020) 3897–3911, https://doi.org/10.1007/s00170-019-04913-6.
[5] M.E. Korkmaz, M.K. Gupta, E. Çelik, N.S. Ross, M. Günay, A sustainable cooling/lubrication method focusing on energy consumption and other machining characteristics in high-speed turning of aluminum alloy, Sustain. Mater. Technol. 40 (Jul. 2024) e00919, https://doi.org/10.1016/J.SUSMAT.2024.E00919.
[6] K. Kumar, D. Zindani, J.P. Davim, Introduction to Machining Processes, 2018.
[7] E.M. Trent, P.K. Wright, Metal Cutting Fourth Edition, 2000.
[8] Y. Wang, T. Toly, T. Chen, ScienceDirect an FNLP approach for planning energy-efficient manufacturing: wafer fabricationas an example, Procedia Manuf. 38 (2019) 439–446, https://doi.org/10.1016/j.promfg.2020.01.056, 2020.
[9] Z. Wang, L. Li, Optimization of process parameters for surface roughness and tool wear in milling TC17 alloy using Taguchi with grey relational analysis, Adv. Mech. Eng. 13 (2) (2021) 1–8, https://doi.org/10.1177/1687814021996530.
[10] M.A. Khan, et al., Statistical analysis of energy consumption, tool wear and surface roughness in machining of Titanium alloy (Ti-6Al-4V) under dry, wet and cryogenic conditions, Mech. Sci. 10 (2) (2019) 561–573, https://doi.org/10.5194/ms-10-561-2019.
[11] Z. Zhu, X. Guo, M. Ekevad, P. Cao, B. Na, N. Zhu, The effects of cutting parameters and tool geometry on cutting forces and tool wear in milling high-density fiberboard with ceramic cutting tools, Int. J. Adv. Manuf. Technol. 91 (9–12) (2017) 4033–4041, https://doi.org/10.1007/s00170-017-0085-8.
[12] S.I. Jaffery, N. Driver, P.T. Mativenga, Analysis of process parameters in the micromachining of Ti-6Al-4V alloy, Proc. 36th Int. MATADOR Conf. 2010-Janua (2010) 239–242, https://doi.org/10.1007/978-1-84996-432-6_55.
[13] Gilbert, W. W, Economics of machining, Mach. Pract (1950) 465–485.
[14] J. Xie, et al., Phase transformation mechanisms of NiTi shape memory alloy during electromagnetic pulse welding of Al/NiTi dissimilar joints, Mater. Sci. Eng. A 893 (Feb. 2024) 146119, https://doi.org/10.1016/J.MSEA.2024.146119.
[15] D. Xiao, et al., Model for economic evaluation of closed-loop geothermal systems based on net present value, Appl. Therm. Eng. 231 (Aug. 2023) 121008, https://doi.org/10.1016/J.APPLTHERMALENG.2023.121008.

[16] L. Hu, et al., Minimising the machining energy consumption of a machine tool by sequencing the features of a part, Energy 121 (2017) 292–305, https://doi.org/10.1016/j.energy.2017.01.039.
[17] W. Cai, F. Liu, X.N. Zhou, J. Xie, Fine energy consumption allowance of workpieces in the mechanical manufacturing industry, Energy 114 (2016) 623–633, https://doi.org/10.1016/j.energy.2016.08.028.
[18] L. Hu, et al., Sequencing the features to minimise the non-cutting energy consumption in machining considering the change of spindle rotation speed, Energy 139 (2017) 935–946, https://doi.org/10.1016/j.energy.2017.08.032.
[19] Q. Wang, F. Liu, C. Li, An integrated method for assessing the energy efficiency of machining workshop, J. Clean. Prod. 52 (2013) 122–133, https://doi.org/10.1016/j.jclepro.2013.03.020. September 2009.
[20] T. Gutowski, J. Dahmus, A. Thiriez, Electrical Energy Requirements for Manufacturing Processes, 2006 no. Cvd.
[21] F. Draganescu, M. Gheorghe, C. V Doicin, Models of Machine Tool Efficiency and Specific Consumed Energy, 141, 2003, pp. 9–15. September 2002.
[22] S.T. Newman, A. Nassehi, V. Dhokia, CIRP journal of manufacturing science and technology energy efficient process planning for CNC machining, CIRP J. Manuf. Sci. Technol. 5 (2) (2012) 127–136, https://doi.org/10.1016/j.cirpj.2012.03.007.
[23] L. Zhou, F. Li, F. Zhao, J. Li, J.W. Sutherland, Characterizing the effect of process variables on energy consumption in end milling, Int. J. Adv. Manuf. Technol. 101 (9–12) (2019) 2837–2848, https://doi.org/10.1007/s00170-018-3015-5.
[24] J.G. Li, Y. Lu, H. Zhao, P. Li, Y.X. Yao, Optimization of cutting parameters for energy saving, Int. J. Adv. Manuf. Technol. 70 (1–4) (2014) 117–124, https://doi.org/10.1007/s00170-013-5227-z.
[25] J. Li, Z. Wang, S. Zhang, Y. Lin, L. Jiang, J. Tan, Task incremental learning-driven Digital-Twin predictive modeling for customized metal forming product manufacturing process, Robot. Comput. Integrated Manuf. 85 (Feb. 2024) 102647, https://doi.org/10.1016/J.RCIM.2023.102647.
[26] Y. Xiang, Z. Wang, S. Zhang, L. Jiang, Y. Lin, J. Tan, Cross-sectional performance prediction of metal tubes bending with tangential variable boosting based on parameters-weight-adaptive CNN, Expert Syst. Appl. 237 (Mar. 2024) 121465, https://doi.org/10.1016/J.ESWA.2023.121465.
[27] L. Zhu et al., "Effect of Cold Spray Parameters on Surface Roughness, Thickness and Adhesion of Copper Based Composite Coating on Aluminium Alloy 6061 T6 Substrate," doi: 10.2139/SSRN.4369202.
[28] X. Zhang, T. Yu, W. Wang, Prediction of cutting forces and instantaneous tool deflection in micro end milling by considering tool run-out, Int. J. Mech. Sci. 136 (Feb. 2018) 124–133, https://doi.org/10.1016/j.ijmecsci.2017.12.019.
[29] Z. Zhou, D. Chen, S. Shengquan, Xie, Springer Series in Advanced Manufacturing, 2007.
[30] C. Wu, B. Li, Y. Liu, S.Y. Liang, Surface roughness modeling for grinding of Silicon Carbide ceramics considering co-existence of brittleness and ductility, Int. J. Mech. Sci. 133 (Nov. 2017) 167–177, https://doi.org/10.1016/j.ijmecsci.2017.07.061.
[31] B. Wang, Z. Liu, Q. Song, Y. Wan, Z. Shi, Proper selection of cutting parameters and cutting tool angle to lower the specific cutting energy during high speed machining of 7050-T7451 aluminum alloy, J. Clean. Prod. 129 (Aug. 2016) 292–304, https://doi.org/10.1016/j.jclepro.2016.04.071.
[32] M.A. Khan, S.H.I. Jaffery, M. Khan, Assessment of sustainability of machining Ti-6Al-4V under cryogenic condition using energy map approach, Engineering Science and Technology, an International Journal 41 (2023) 101357.
[33] M. Sheheryar, et al., Multi-objective optimization of process parameters during micro-milling of nickel-based alloy inconel 718 using taguchi-grey relation integrated approach, Materials 15 (23) (2022), https://doi.org/10.3390/ma15238296.
[34] M.A.M. Khan, S. Husain Imran Jaffery, M.A.M. Khan, R. Ahmad, S.I. Butt, Sustainability analysis of turning aerospace alloy Ti-6Al-4V under dry, wet and cryogenic conditions, Proc. 2020 IEEE 11th Int. Conf. Mech. Intell. Manuf. Technol. ICMIMT (2020) 27–30, https://doi.org/10.1109/ICMIMT49010.2020.9041160, 2020.
[35] A. Ahmad, et al., Achieving sustainable machining of titanium grade 3 alloy through optimization using grey relational analysis (GRA), Results Eng 23 (May) (2024) 102355, https://doi.org/10.1016/j.rineng.2024.102355.
[36] S.R.S. Serope Kalpakjian, Manufacturing Engineering and Technology, sixth ed., 2010.
[37] M. Kiliç, E. Burdurlu, S. Aslan, S. Altun, Ö. Tümerdem, The effect of surface roughness on tensile strength of the medium density fiberboard (MDF) overlaid with polyvinyl chloride (PVC), Mater. Des. 30 (10) (Dec. 2009) 4580–4583, https://doi.org/10.1016/j.matdes.2009.03.029.
[38] A. Javidi, U. Rieger, W. Eichlseder, The effect of machining on the surface integrity and fatigue life, Int. J. Fatig. 30 (10–11) (Oct. 2008) 2050–2055, https://doi.org/10.1016/j.ijfatigue.2008.01.005.
[39] P. Mikell, Groover Fundamentals of Modern Manufacturing Materials, Processes, and Systems, Fourth Edition 2010.pdf, 2016, pp. 1–1028.
[40] M.A. Khan, et al., Experimental evaluation of surface roughness, burr formation, and tool wear during micro-milling of titanium grade 9 (Ti-3Al-2.5V) using statistical evaluation methods, Appl. Sci. 13 (23) (2023), https://doi.org/10.3390/app132312875.
[41] M.A. Khan, S.H.I. Jaffery, M.A. Khan, M.I. Faraz, S. Mufti, Multi-objective optimization of micro-milling titanium alloy Ti-3Al-2.5V (grade 9) using taguchi-grey relation integrated approach, Metals 13 (8) (2023), https://doi.org/10.3390/met13081373.
[42] A. Baig, S.H.I. Jaffery, M.A. Khan, M. Alruqi, Statistical analysis of surface roughness, burr formation and tool wear in high speed micro milling of inconel 600 alloy under cryogenic, wet and dry conditions, Micromachines 14 (1) (2023), https://doi.org/10.3390/mi14010013.
[43] J. Beddoes, M.J. Bibby, Metal processing and manufacturing, in: Principles of Metal Manufacturing Processes, Elsevier, 1999, pp. 1–17.
[44] T.T. Nguyen, Prediction and optimization of machining energy, surface roughness, and production rate in SKD61 milling, Meas. J. Int. Meas. Confed. 136 (January) (Mar. 2019) 525–544, https://doi.org/10.1016/j.measurement.2019.01.009.
[45] M.Y. Wang, H.Y. Chang, Experimental study of surface roughness in slot end milling AL2014-T6, Int. J. Mach. Tool Manufact. 44 (1) (Jan. 2004) 51–57, https://doi.org/10.1016/j.ijmachtools.2003.08.011.
[46] D. Nathan, D. Elilraja, T. Prabhuram, S. Prathap Singh, Experimental investigation of surface roughness in end milling of AA6061 alloy with flooded cooling and minimum quantity lubrication (MQL) technique, Lect. Notes Mech. Eng. (2021) 649–659, https://doi.org/10.1007/978-981-15-4745-4_58.
[47] A. Muhammad, M.K. Gupta, T. Mikołajczyk, D.Y. Pimenov, K. Giasin, Effect of tool coating and cutting parameters on surface roughness and burr formation during micromilling of inconel 718, Metals 11 (1) (Jan. 2021) 1–18, https://doi.org/10.3390/met11010167.
[48] C. Camposeco-Negrete, Optimization of cutting parameters using Response Surface Method for minimizing energy consumption and maximizing cutting quality in turning of AISI 6061 T6 aluminum, J. Clean. Prod. 91 (2015) 109–117, https://doi.org/10.1016/j.jclepro.2014.12.017.
[49] M. Ali Khan, S. Husain Imran Jaffery, M. Khan, S. Ikramullah Butt, Wear and surface roughness analysis of machining of Ti-6Al-4V under dry, wet and cryogenic conditions, IOP Conf. Ser. Mater. Sci. Eng. 689 (1) (2019) 2–7, https://doi.org/10.1088/1757-899X/689/1/012006.
[50] N. Liu, S.B. Wang, Y.F. Zhang, W.F. Lu, A novel approach to predicting surface roughness based on specific cutting energy consumption when slot milling Al-7075, Int. J. Mech. Sci. 118 (Nov. 2016) 13–20, https://doi.org/10.1016/j.ijmecsci.2016.09.002.
[51] R. Sanjeevi, R. Nagaraja, B. Radha Krishnan, "Vision-based surface roughness accuracy prediction in the CNC milling process (Al6061) using ANN,", Mater. Today Proc. (2020) https://doi.org/10.1016/j.matpr.2020.05.122.
[52] G. Ul Rehman, S. Husain Imran Jaffery, M. Khan, L. Ali, A. Khan, S. Ikramullah Butt, Analysis of burr formation in low speed micro-milling of titanium alloy (Ti-6Al-4V), Mech. Sci. 9 (2) (Jul. 2018) 231–243, https://doi.org/10.5194/ms-9-231-2018.
[53] S. Saha, A. Sravan Kumar, S. Deb, P.P. Bandyopadhyay, An investigation on the top burr formation during Minimum Quantity Lubrication (MQL) assisted micromilling of copper, Mater. Today Proc. 26 (Jan. 2020) 1809–1814, https://doi.org/10.1016/J.MATPR.2020.02.379.
[54] S.L. Ko, J.K. Lee, Analysis of burr formation in drilling with a new-concept drill, J. Mater. Process. Technol. 113 (1–3) (2001) 392–398, https://doi.org/10.1016/S0924-0136(01)00717-8.
[55] C. Yuhua, M. Yuqing, L. Weiwei, H. Peng, Investigation of welding crack in micro laser welded NiTiNb shape memory alloy and Ti6Al4V alloy dissimilar metals joints, Opt. Laser Technol. 91 (Jun. 2017) 197–202, https://doi.org/10.1016/J.OPTLASTEC.2016.12.028.
[56] Y. Liu, Y. Liu, T. Wang, Z. Wang, Q. Huang, Mathematical modeling and analysis of the tailor rolled blank manufacturing process, Int. J. Mech. Sci. 266 (Mar. 2024) 108991, https://doi.org/10.1016/J.IJMECSCI.2024.108991.
[57] M. Kumar, V. Bajpai, "Experimental investigation of top burr formation in high-speed micro-milling of Ti6Al4V alloy:," 234 (4) (2019) 730–738, https://doi.org/10.1177/0954405419883049. Oct.

[58] W. Zhao, H. Wang, W. Chen, Studying the effects of cutting parameters on burr formation and deformation of hierarchical micro-structures in ultra-precision raster milling, Int. J. Adv. Manuf. Technol. 101 (5–8) (Apr. 2019) 1133–1141, https://doi.org/10.1007/s00170-018-3003-9.
[59] S.A. Niknam, V. Songmene, Statistical Investigation on Burrs Thickness during Milling of 6061-T6 Aluminium Alloy, 2012.
[60] G.M. Schueler, et al., Burrs - analysis, control and removal, Burrs - Anal. Control Remov (2010), https://doi.org/10.1007/978-3-642-00568-8.
[61] M. Takács, B. Verö, I. Mészáros, Micromilling of metallic materials, J. Mater. Process. Technol. 138 (1–3) (2003) 152–155, https://doi.org/10.1016/S0924-0136(03)00064-5.
[62] J. Schmidt, H. Tritschler, Micro cutting of steel, Microsyst. Technol. 10 (3) (2004) 167–174, https://doi.org/10.1007/s00542-003-0346-3.
[63] S.H.I. Jaffery, M. Khan, L. Ali, P.T. Mativenga, Statistical analysis of process parameters in micromachining of Ti-6Al-4V alloy, Proc. Inst. Mech. Eng. Part B J. Eng. Manuf. 230 (6) (2016) 1017–1034, https://doi.org/10.1177/0954405414564409.
[64] G.K. Mathai, S.N. Melkote, D.W. Rosen, Effect of process parameters on burrs produced in micromilling of a thin nitinol foil, J. Micro Nano-Manufacturing 1 (2) (2013) 1–10, https://doi.org/10.1115/1.4024099.
[65] N. Swain, V. Venkatesh, P. Kumar, G. Srinivas, S. Ravishankar, H.C. Barshilia, An experimental investigation on the machining characteristics of Nimonic 75 using uncoated and TiAlN coated tungsten carbide micro-end mills, CIRP J. Manuf. Sci. Technol. 16 (Jan. 2017) 34–42, https://doi.org/10.1016/J.CIRPJ.2016.07.005.
[66] E. Kuram, Tool coating effect on the performance in milling of Al2124 aluminium alloy, Dokuz Eylül Üniversitesi Mühendislik Fakültesi Fen ve Mühendislik Derg. 21 (63) (Sep. 2019) 749–760, https://doi.org/10.21205/DEUFMD.2019216307.
[67] P. Kumar, M. Kumar, V. Bajpai, N.K. Singh, Recent advances in characterization, modeling and control of burr formation in micro-milling, Manuf. Lett. 13 (Aug. 2017) 1–5, https://doi.org/10.1016/J.MFGLET.2017.04.002.
[68] A. Rauf, M.A. Khan, S.H.I. Jaffery, S.I. Butt, Effects of machining parameters, ultrasonic vibrations and cooling conditions on cutting forces and tool wear in meso scale ultrasonic vibrations assisted end-milling (UVAEM) of Ti-6Al-4V under dry, flooded, MQL and cryogenic environments–A statistical analysis, J. Mater. Res. Technol. 30 (2024) 8287–8303. https://doi.org/10.1016/j.jmrt.2024.05.202.
[69] X. Chen, C. Li, Y. Tang, L. Li, Y. Du, L. Li, Integrated optimization of cutting tool and cutting parameters in face milling for minimizing energy footprint and production time, Energy 175 (2019) 1021–1037, https://doi.org/10.1016/j.energy.2019.02.157.
[70] A.M. Khan, et al., Multi-objective optimization of energy consumption and surface quality in nanofluid SQCL assisted face milling, Energies 12 (4) (2019) 710, https://doi.org/10.3390/EN12040710, 710, Feb. 2019.
[71] D.Y. Pimenov, A.T. Abbas, M.K. Gupta, I.N. Erdakov, M.S. Soliman, M.M. El Rayes, Investigations of surface quality and energy consumption associated with costs and material removal rate during face milling of AISI 1045 steel, Int. J. Adv. Manuf. Technol. 107 (7–8) (2020) 3511–3525, https://doi.org/10.1007/s00170-020-05236-7.
[72] G.R. Singh, M.K. Gupta, M. Mia, V.S. Sharma, Modeling and optimization of tool wear in MQL-assisted milling of Inconel 718 superalloy using evolutionary techniques, Int. J. Adv. Manuf. Technol. 97 (1–4) (2018) 481–494, https://doi.org/10.1007/s00170-018-1911-3.
[73] M. Younas, et al., Multi-objective optimization for sustainable turning Ti6Al4V alloy using grey relational analysis (GRA) based on analytic hierarchy process (AHP), Int. J. Adv. Manuf. Technol. 105 (1–4) (2019) 1175–1188, https://doi.org/10.1007/s00170-019-04299-5.
[74] M.A. Khan, S.H. Imran Jaffery, M. Khan, M. Alruqi, Machinability analysis of Ti-6Al-4V under cryogenic condition, J. Mater. Res. Technol. 25 (2023) 2204–2226, https://doi.org/10.1016/j.jmrt.2023.06.022.
[75] M.A. Khan, S.H.I. Jaffery, A.A. Baqai, M. Khan, Comparative analysis of tool wear progression of dry and cryogenic turning of titanium alloy Ti-6Al-4V under low, moderate and high tool wear conditions, Int. J. Adv. Manuf. Technol. 121 (1–2) (2022) 1269–1287, https://doi.org/10.1007/s00170-022-09196-y.
[76] S.I. Jaffery, P.T. Mativenga, Study of the use of wear maps for assessing machining performance, Proc. Inst. Mech. Eng. Part B J. Eng. Manuf. 223 (9) (2009) 1097–1105, https://doi.org/10.1243/09544054JEM1462.
[77] K.N. Shi, D.H. Zhang, N. Liu, S.B.L. Wang, J.X. Ren, S.B.L. Wang, A novel energy consumption model for milling process considering tool wear progression, J. Clean. Prod. 184 (May 2018) 152–159, https://doi.org/10.1016/j.jclepro.2018.02.239.
[78] Z.Q.Y. Liu, Y.B. Guo, M.P. Sealy, Z.Q.Y. Liu, Energy consumption and process sustainability of hard milling with tool wear progression, J. Mater. Process. Technol. 229 (2016) 305–312, https://doi.org/10.1016/j.jmatprotec.2015.09.032.
[79] J. Budd, The adsorption of aluminium from aqueous solution by cellulose fibres, Colloids and surfaces 41 (1989) 363–384.
[80] D. Ashkenazi, How aluminum changed the world: a metallurgical revolution through technological and cultural perspectives, Technol. Forecast. Soc. Change 143 (June 2018) 101–113, https://doi.org/10.1016/j.techfore.2019.03.011. Jun. 2019.
[81] S. Wang, et al., The design of low-temperature solder alloys and the comparison of mechanical performance of solder joints on ENIG and ENEPIG interface, J. Mater. Res. Technol. 27 (Nov. 2023) 5332–5339, https://doi.org/10.1016/J.JMRT.2023.11.066.
[82] A.S. Warren, Developments and challenges for aluminum - a boeing perspective, Mater. Forum 28 (2004) 24–31.
[83] M. Nouari, B. Haddag, A. Moufki, S. Atlati, Investigation on the Built-Up Edge Process when Dry Machining Aeronautical Aluminum Alloys, Mach. Light Alloy, Aug. 2018, pp. 35–48, https://doi.org/10.1201/B22153-2.
[84] A. Gómez-Parra, M. Álvarez-Alcón, J. Salguero, M. Batista, M. Marcos, Analysis of the evolution of the Built-Up Edge and Built-Up Layer formation mechanisms in the dry turning of aeronautical aluminium alloys, Wear 302 (1–2) (Apr. 2013) 1209–1218, https://doi.org/10.1016/J.WEAR.2012.12.001.
[85] X. Zhang, T. Yu, Y. Dai, S. Qu, J. Zhao, Energy consumption considering tool wear and optimization of cutting parameters in micro milling process, Int. J. Mech. Sci. 178 (March) (Jul. 2020) 105628, https://doi.org/10.1016/j.ijmecsci.2020.105628.
[86] S.S. Warsi, et al., Development of energy consumption map for orthogonal machining of Al 6061-T6 alloy, Proc. Inst. Mech. Eng. Part B J. Eng. Manuf. 232 (14) (Apr. 2018) 2510–2522, https://doi.org/10.1177/0954405417703424.
[87] S.Y. Jin, A. Pramanik, A.K. Basak, C. Prakash, S. Shankar, S. Debnath, Burr formation and its treatments—a review, Int. J. Adv. Manuf. Technol. 107 (5–6) (2020) 2189–2210, https://doi.org/10.1007/s00170-020-05203-2.
[88] M. Luo, G. Liu, M. Chen, Mechanism of burr formation and control methods in slot milling Al-alloy, Shanghai Jiaotong Daxue Xuebao/Journal Shanghai Jiaotong Univ. 41 (12) (2007) 1905–1909.
[89] S. Hajiahmadi, Burr size investigation in micro milling of stainless steel 316L, Int. J. Light. Mater. Manuf. 2 (4) (Dec. 2019) 296–304, https://doi.org/10.1016/J.IJLMM.2019.07.004.
[90] S.S. Warsi, H.I. Jaffery, R. Ahmad, M. Khan, S. Akram, Analysis of Power and Specific Cutting Energy Consumption in Orthogonal Machining of Al 6061-T6 Alloys at Transitional Cutting Speeds, 2016, https://doi.org/10.1115/imece2015-53290. V02BT02A057.
[91] S.R. Zaidi, N. Ul Qadir, S.H.I. Jaffery, M.A. Khan, M. Khan, J. Petru, Statistical analysis of machining parameters on burr formation, surface roughness and energy consumption during milling of aluminium alloy Al 6061-T6, Materials 15 (22) (2022), https://doi.org/10.3390/ma15228065.
[92] T. Gutowski, et al., Environmentally benign manufacturing: observations from Japan, europe and the United States, J. Clean. Prod. 13 (1) (2005) 1–17, https://doi.org/10.1016/j.jclepro.2003.10.004.
[93] A.I. Gusri, B. Yanuar, M.S.A. Yasir, BURR FORMATION ANALYSIS WHEN MICRO MILLING Ti-6Al-4V ELI USING END MILL CARBIDE INSERT, PalArch's J. Archaeol. Egypt 17 (9) (2020) 4061–4067.
[94] M. Ap, "CoroMill ® 390 Shoulder Milling Body Tailor Made Offer (Metric)," no. Dc, pp. 2–7..
[95] Y.Y. Genichi Taguchi, Taguchi Methods: Design of Experiments (TAGUCHI METHODS SERIES), Amer Supplier Inst, 1993.
[96] T.R. Bement, Taguchi techniques for quality engineering, Technometrics 31 (2) (1989) 253–255, https://doi.org/10.1080/00401706.1989.10488519.
[97] P.J. Ross, Taguchi techniques for quality engineering: loss function, orthogonal experiments, parameter and tolerance design, Loss Fuction, Orthogonal Exp. Param. Toler. Des. 5 (1995) 1–73.
[98] S.R. Zaidi, M. Khan, S.H.I. Jaffery, S.S. Warsi, Effect of machining parameters on surface roughness during milling operation, Advances in Transdisciplinary Engineering 0 (2021) 175–180, https://doi.org/10.3233/atde210033.
[99] J. Melorose, R. Perroy, S. Careas, The influence of number of inserts and cutting parameters on surface roughness in face milling, Statew. Agric. L. Use Baseline 1 (1) (2015) 1–7, 2015.

[100] J.P. Davim, V.P. Astakhov, Machining of Hard Metals, 2011.
[101] D.A. Axinte, R.C. Dewes, Surface integrity of hot work tool steel after high speed milling-experimental data and empirical models, J. Mater. Process. Technol. 127 (3) (Oct. 2002) 325–335, https://doi.org/10.1016/S0924-0136(02)00282-0.
[102] M. Sarỳkaya, H. Dilipak, A. Gezgin, Optimization of the process parameters for surface roughness and tool life in face milling using the Taguchi analysis, Mater. Tehnol. 49 (1) (2015) 139–147.
[103] S. Jeyakumar, K. Marimuthu, T. Ramachandran, Prediction of cutting force, tool wear and surface roughness of Al6061/SiC composite for end milling operations using RSM, J. Mech. Sci. Technol. 27 (9) (2013) 2813–2822, https://doi.org/10.1007/s12206-013-0729-z.
[104] T.H. Pham, D.T. Nguyen, T.L. Banh, V.C. Tong, Experimental study on the chip morphology, tool–chip contact length, workpiece vibration, and surface roughness during high-speed face milling of A6061 aluminum alloy, Proc. Inst. Mech. Eng. Part B J. Eng. Manuf. 234 (3) (Feb. 2020) 610–620, https://doi.org/10.1177/0954405419863221.
[105] B. Öztürk, L. Uğur, A. Yildiz, Investigation of effect on energy consumption of surface roughness in X-axis and spindle servo motors in slot milling operation, Measurement 139 (2019) 92–102, https://doi.org/10.1016/j.measurement.2019.02.009.
[106] C. Zhang, W. Li, P. Jiang, P. Gu, Experimental investigation and multi-objective optimization approach for low-carbon milling operation of aluminum, Proc. Inst. Mech. Eng. Part C J. Mech. Eng. Sci. 231 (15) (Mar. 2017) 2753–2772, https://doi.org/10.1177/0954406216640574.
[107] S. Akram, S.H.I. Jaffery, M. Khan, M. Fahad, A. Mubashar, L. Ali, Numerical and experimental investigation of Johnson–Cook material models for aluminum (AL 6061-t6) alloy using orthogonal machining approach, Adv. Mech. Eng. 10 (9) (2018) 1–14, https://doi.org/10.1177/1687814018797794.
[108] Y. Cao, C. Wang, Y. Ping, P. Hou, W. Wu, An experimental study on burrs in micro milling antenna micro narrow slots. Proc. 2019 IEEE Int. Conf. Mechatronics Autom, ICMA, 2019, pp. 1–5, https://doi.org/10.1109/ICMA.2019.8816498. Aug. 2019.
[109] L.C. Silva, M.B. da Silva, Investigation of burr formation and tool wear in micromilling operation of duplex stainless steel, Precis. Eng. 60 (Nov. 2019) 178–188, https://doi.org/10.1016/J.PRECISIONENG.2019.08.006.
[110] J. Tudela, M. Martínez, R. Valdivia, J. Romo, M. Portillo, R. Rangel, Research on the Modeling of Burr Formation Process in Micro-ball End Milling Operation on Ti-6Al-4V," Nature 388, Springer-Verlag London Ltd, 2012, pp. 539–547, https://doi.org/10.1007/s00170-011-3865-6.
[111] E. Nas, H. Demir, Technology the Influence of Number of Inserts and Cutting, January 2010, 2016.
[112] I. Daniyan, I. Tlhabadira, K. Mpofu, A. Adeodu, Investigating the geometrical effects of cutting tool on the surface roughness of titanium alloy (Ti6Al4V) during milling operation, Procedia CIRP 99 (2021) 157–164, https://doi.org/10.1016/j.procir.2021.03.097.
[113] T. Zhang, Z. Liu, X. Sun, J. Xu, L. Dong, G. Zhu, Investigation on specific milling energy and energy efficiency in high-speed milling based on energy flow theory, Energy 192 (2020), https://doi.org/10.1016/j.energy.2019.116596.
[114] G. Kiswanto, D.L. Zariatin, T.J. Ko, The effect of spindle speed, feed-rate and machining time to the surface roughness and burr formation of Aluminum Alloy 1100 in micro-milling operation, J. Manuf. Process. 16 (4) (Oct. 2014) 435–450, https://doi.org/10.1016/j.jmapro.2014.05.003.
[115] J.C. Aurich, D. Dornfeld, P.J. Arrazola, V. Franke, L. Leitz, S. Min, Burrs-Analysis, control and removal, CIRP Ann. - Manuf. Technol. 58 (2) (2009) 519–542, https://doi.org/10.1016/j.cirp.2009.09.004.
[116] J. Yan, L. Li, Multi-objective optimization of milling parameters-the trade-offs between energy, production rate and cutting quality, J. Clean. Prod. 52 (Aug. 2013) 462–471, https://doi.org/10.1016/j.jclepro.2013.02.030.
[117] C. R. Management, Grey Data Analysis. .
[118] Y. Kuo, T. Yang, G.W. Huang, The use of a grey-based Taguchi method for optimizing multi-response simulation problems, Eng. Optim. 40 (6) (2008) 517–528, https://doi.org/10.1080/03052150701857645.
[119] K. Khanafer, A. Eltaggaz, I. Deiab, H. Agarwal, A. Abdul-latif, Toward sustainable micro-drilling of Inconel 718 superalloy using MQL-Nanofluid, Int. J. Adv. Manuf. Technol. 107 (7–8) (Apr. 2020) 3459–3469, https://doi.org/10.1007/s00170-020-05112-4.
[120] K.V.M.K. Raju, G.R. Janardhana, P.N. Kumar, V.D.P. Rao, Optimization of cutting conditions for surface roughness in CNC end milling, Int. J. Precis. Eng. Manuf. 12 (3) (2011) 383–391, https://doi.org/10.1007/s12541-011-0050-7.
[121] M. Moradnazhad, H.O. Unver, Energy consumption characteristics of turn-mill machining, Int. J. Adv. Manuf. Technol. 91 (5–8) (2017) 1991–2016, https://doi.org/10.1007/s00170-016-9868-6.
[122] A.M. Zain, H. Haron, S. Sharif, Prediction of surface roughness in the end milling machining using Artificial Neural Network, Expert Syst. Appl. 37 (2) (2010) 1755–1768, https://doi.org/10.1016/j.eswa.2009.07.033.
[123] S.S. Warsi, M.H. Agha, R. Ahmad, S.H.I. Jaffery, M. Khan, Sustainable turning using multi-objective optimization: a study of Al 6061 T6 at high cutting speeds, Int. J. Adv. Manuf. Technol. 100 (1–4) (Jan. 2019) 843–855, https://doi.org/10.1007/s00170-018-2759-2.
[124] S. Wojciechowski, R.W. Maruda, G.M. Krolczyk, P. Niesłony, Application of signal to noise ratio and grey relational analysis to minimize forces and vibrations during precise ball end milling, Precis. Eng. 51 (Jan. 2018) 582–596, https://doi.org/10.1016/J.PRECISIONENG.2017.10.014.
[125] S.P.S.S. Sivam, K. Saravanan, N. Harshavardhana, D. Kumaran, Multi response optimization of setting input variables for getting better cylindrical cups in sheet metal spinning of Al 6061 - T6 by Grey relation analysis, Mater. Today Proc. 45 (2) (2021) 1464–1470, https://doi.org/10.1016/j.matpr.2020.07.453.
[126] U. Esme, M. Bayramoglu, Y. Kazancoglu, S. Ozgun, Optimization of weld bead geometry in TIG welding process using grey relation analysis and Taguchi method, Mater. Tehnol. 43 (3) (2009) 143–149.
[127] A. Roushan, A. Bandyopadhyay, S. Banerjee, Multiple performance characteristics optimisation in side and face milling of glass fibre reinforced polyester composite at different weightage of performances by grey relational analysis, Int. J. Mach. Mach. Mater. 19 (1) (2017) 41–56, https://doi.org/10.1504/IJMMM.2017.081187.